Supplamentary for Translocation of Ti_2CO_2 MXene Monolayer Through the Cell Membranes

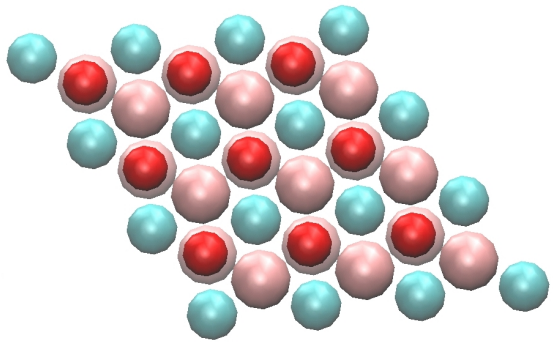

(a) Top view

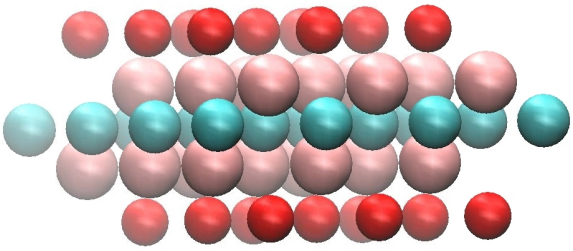

(b) Side view

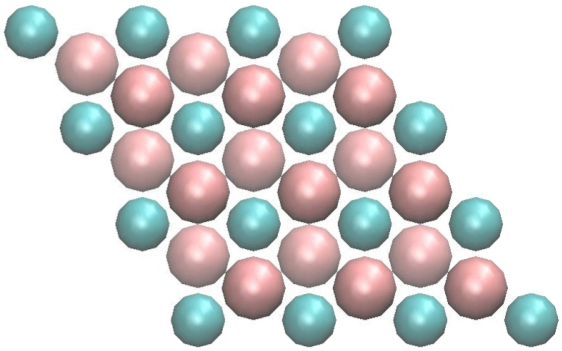

(c) Top view

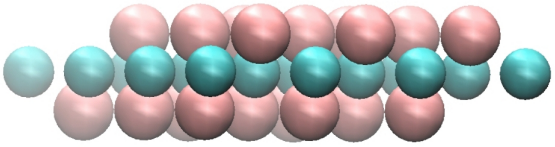

(d) Side view

Figure . S1: Schematic view of all-atom (a), (b) and coarse-grained (c), (d) model of Ti_2CO_2 nanosheet (In the all-atom model: Red beads= Oxygen atoms, Light blue = Carbon atoms, Light pink = Titanium atoms; In the Coarse-Grained model: Light blue = Carbon atoms, Light pink= Merged Titanium and Oxygen atoms)

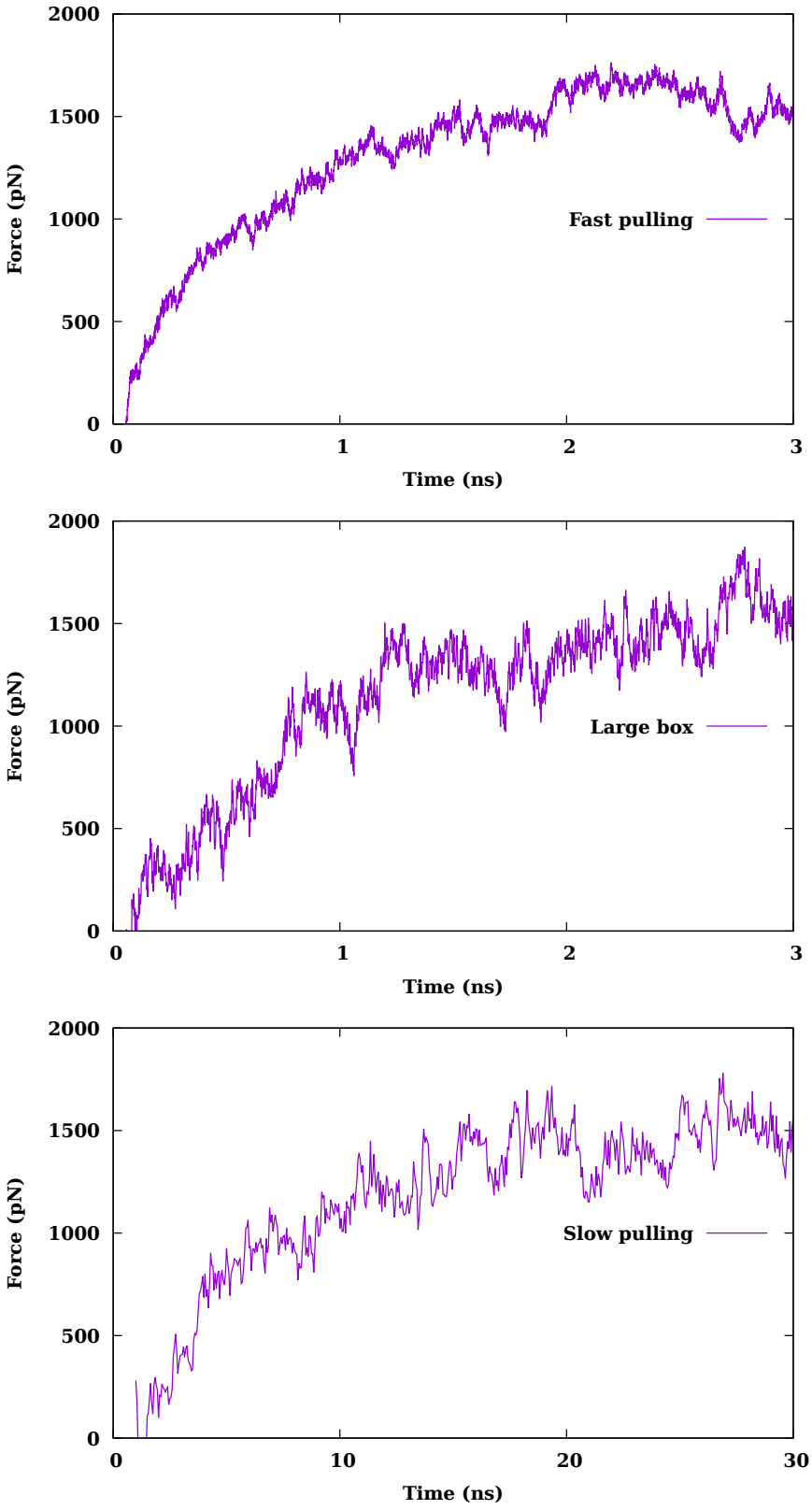

Figure . S2: Comparison of pulling force of three states: Fast pulling speed, 22×10^{-6} Åfs^{-1}, with a box of dimension $160 \times 160 \times 162$ Å^3, Fast pulling speed, 22×10^{-6} Åfs^{-1}, with a box of dimension $320 \times 320 \times 162$ Å^3, Slow pulling speed, 4.4×10^{-6} Åfs^{-1}, with a box of dimension $160 \times 160 \times 162$ Å^3

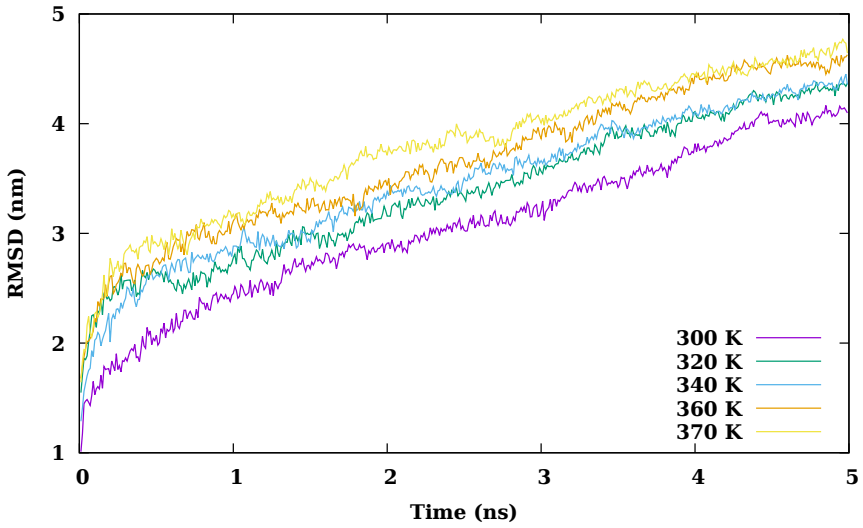

(a)

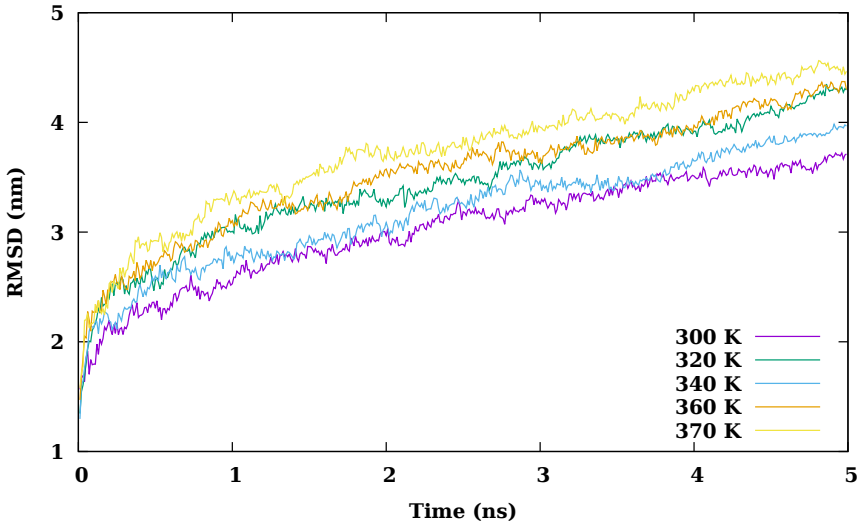

(b)

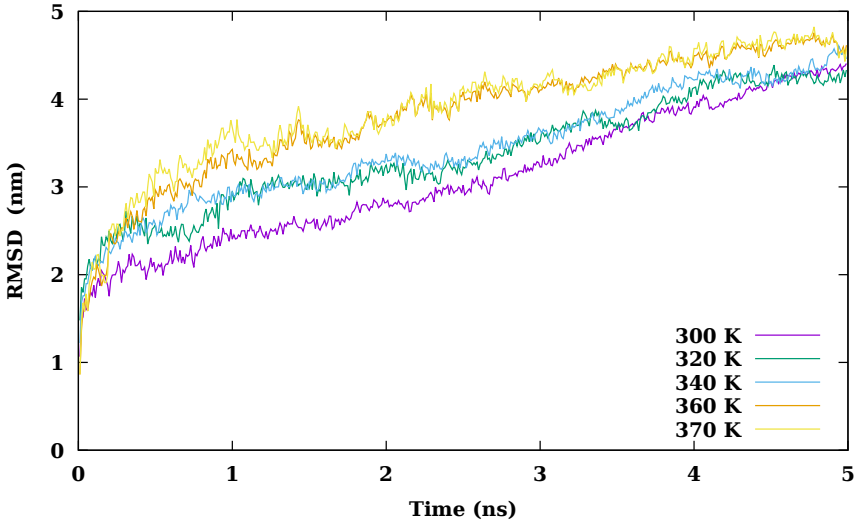

(c)

Figure . S3: Root Mean Square Deviation versus the simulation time at different values of temperature for (a) CF1, (b) CF2 and (c) CF3 configurations.

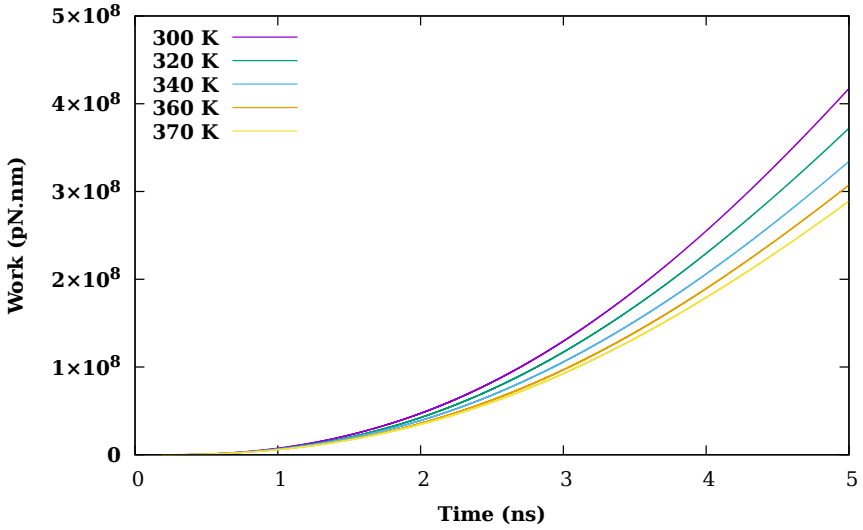

(a)

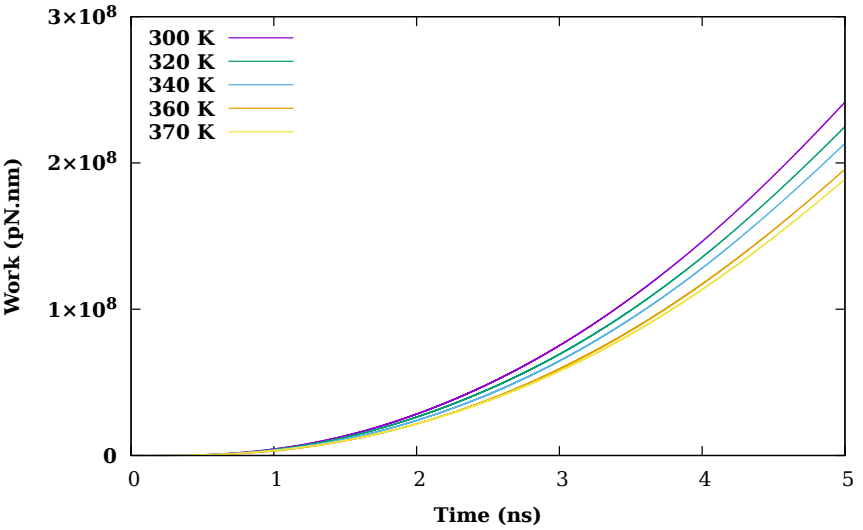

(b)

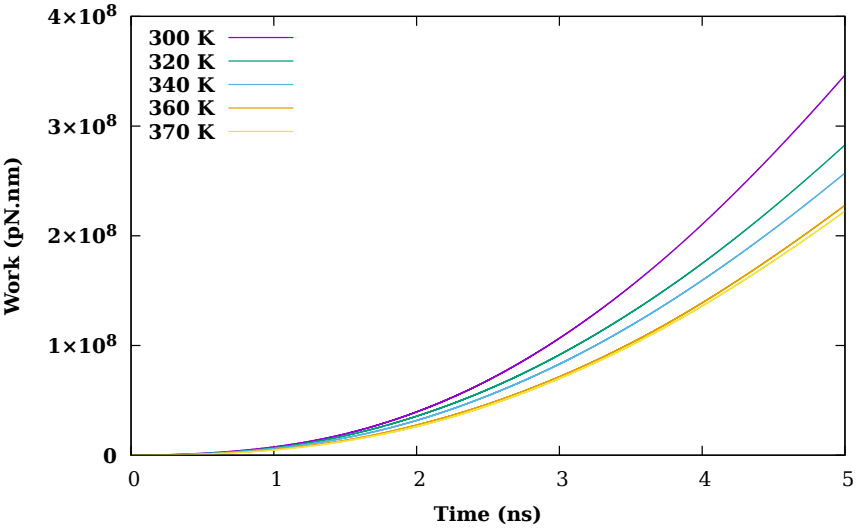

(c)

Figure . S4: Work required to transport the nanosheet through the membrane for (a) CF1, (b) CF2 and (c) CF3 configurations.

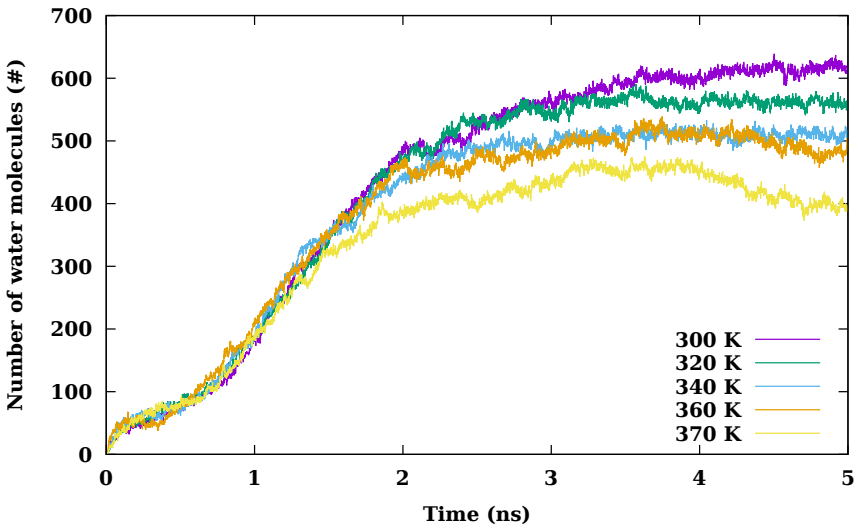

(a)

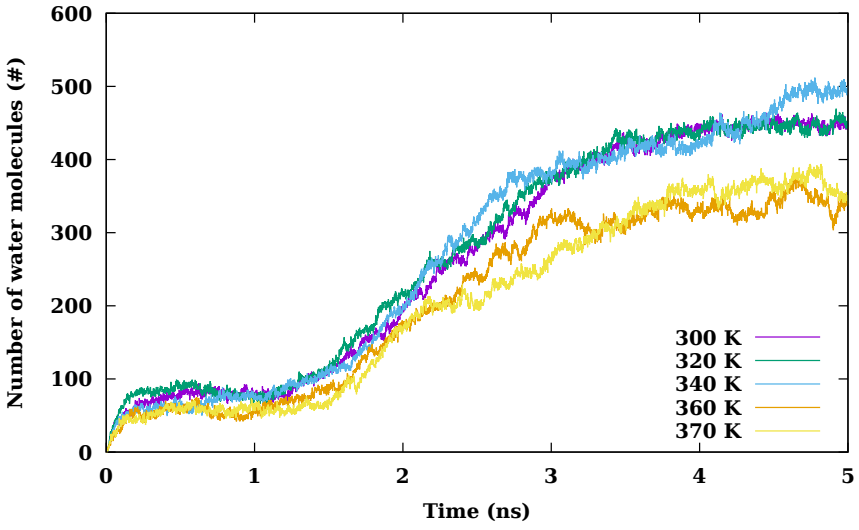

(b)

Figure . S5: Number of water molecules inside cylindrical region of radius 4 nm inside membrane centered at center of nanosheet versus the simulation time at different values of temperature for (a) CF1, (b) CF2 configurations.

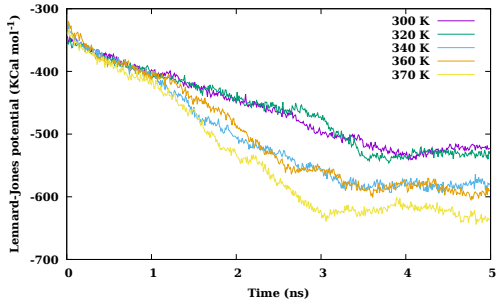

(a) Nanosheet and hydrophilic part of membrane

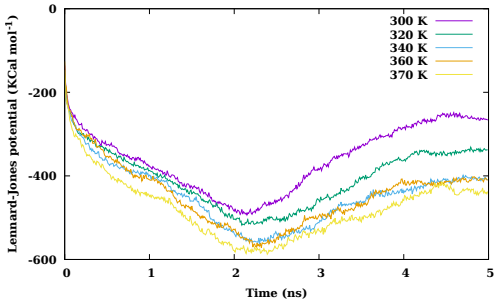

(b) Nanosheet and hydrophilic part of membrane

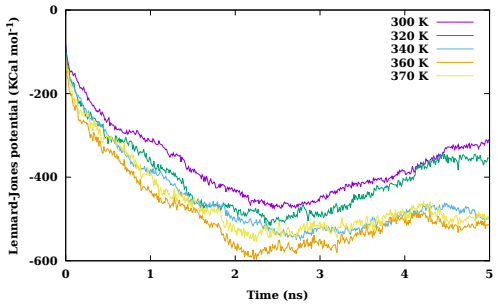

(c) Nanosheet and hydrophilic part of membrane

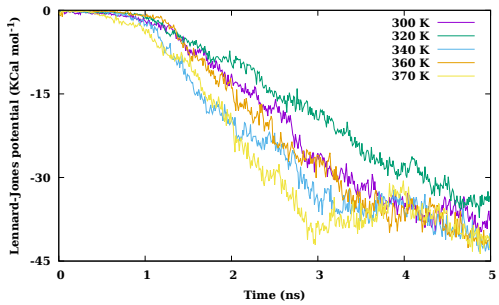

(d) Nanosheet and hydrophobic part of membrane

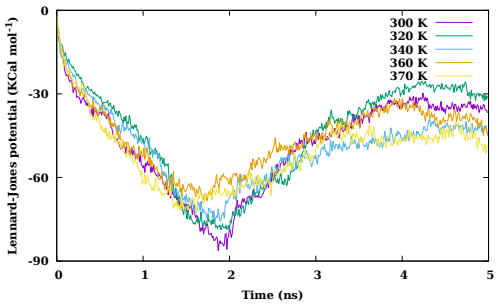

(e) Nanosheet and hydrophobic part of membrane

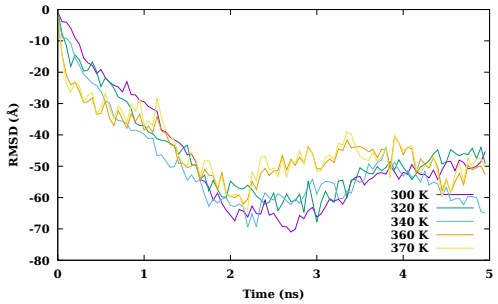

(f) Nanosheet and hydrophobic part of membrane

Figure . S6: Van der Waals interaction between nanosheet and hydrophilic and hydrophobic part of membrane versus the simulation time for (a), (d) CF1, (b), (e) CF2 and (c), (f) CF3 configurations.

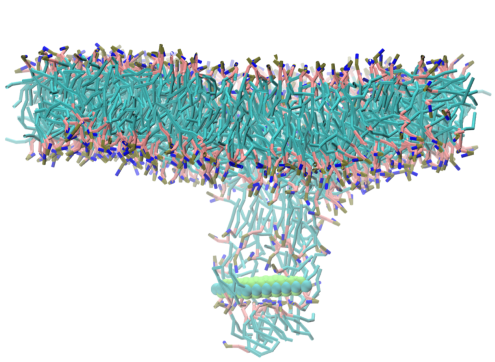

300 K

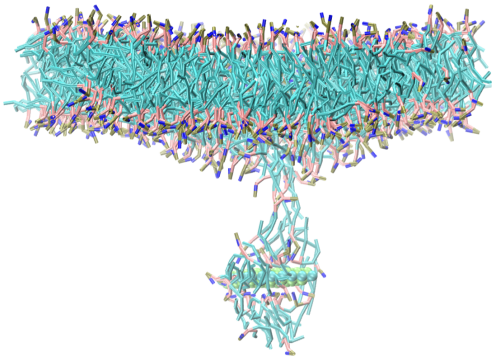

320 K

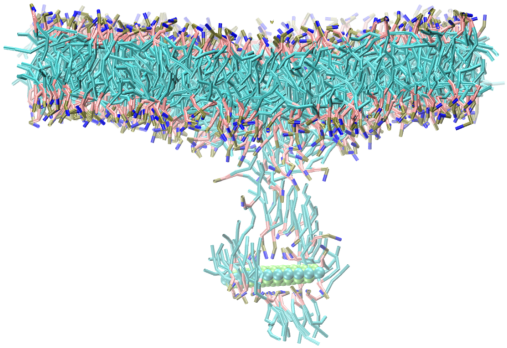

340 K

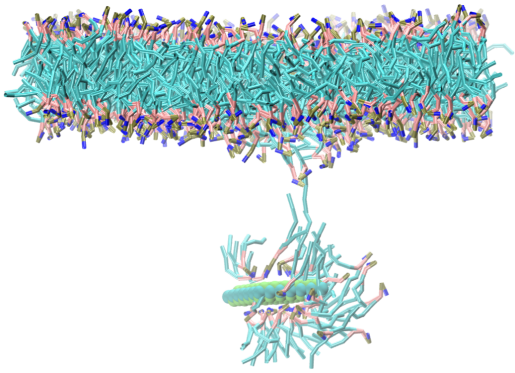

360 K

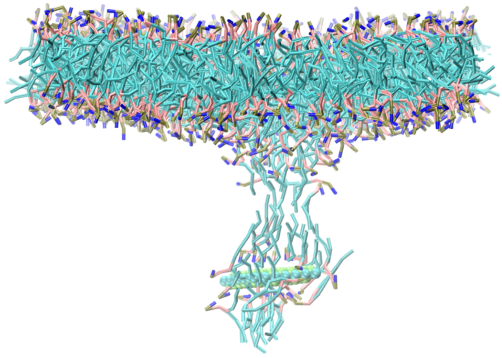

370 K

Figure . S7: Schematic view of final state of CF1 configuration at different values of temperature.

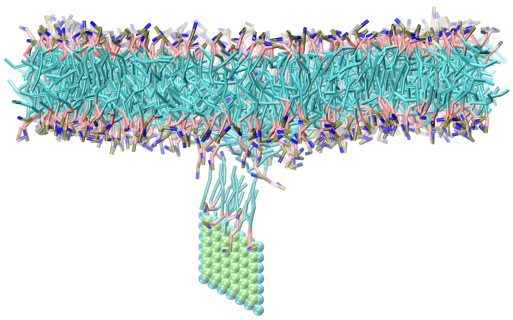

300 K

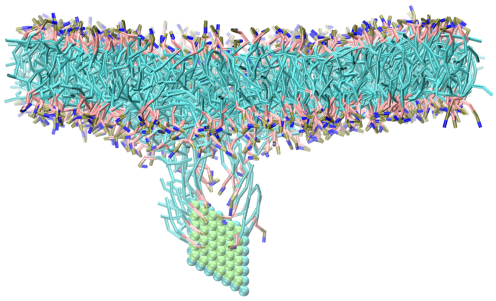

320 K

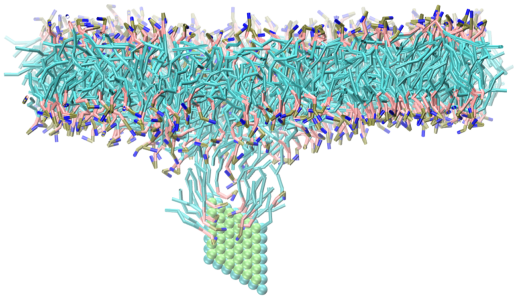

340 K

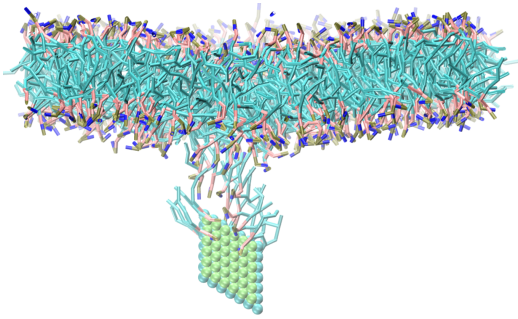

360 K

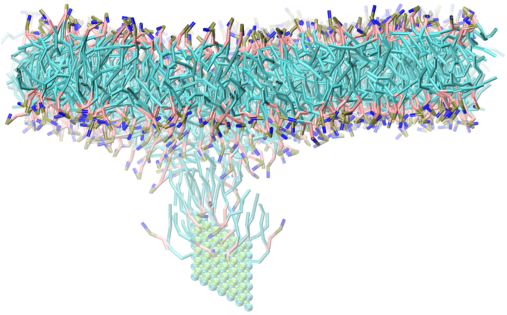

370 K

Figure . S8: Schematic view of final state of CF2 configuration at different values of temperature.

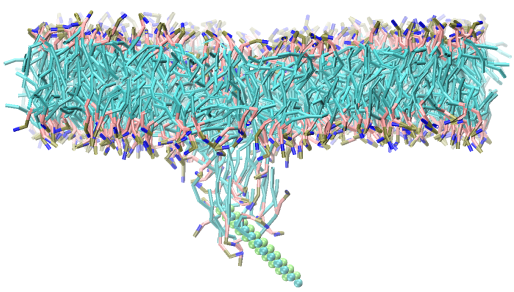

300 K

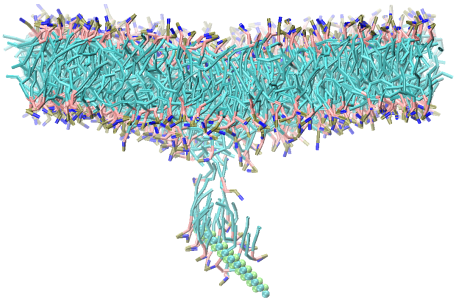

320 K

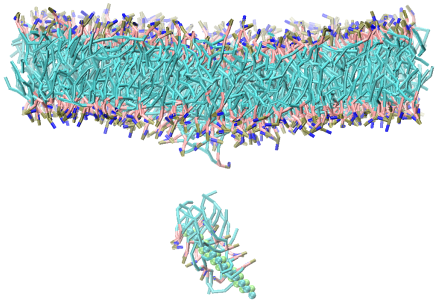

340 K

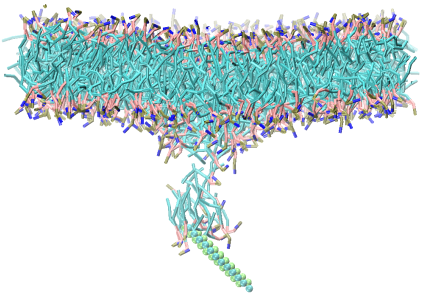

360 K

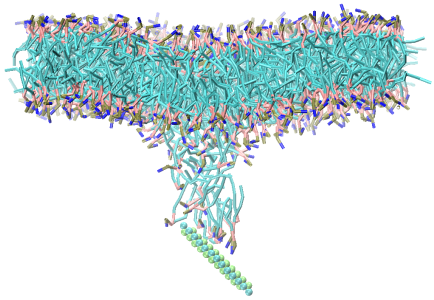

370 K

Figure . S9: Schematic view of final state of CF3 configuration at different values of temperature.

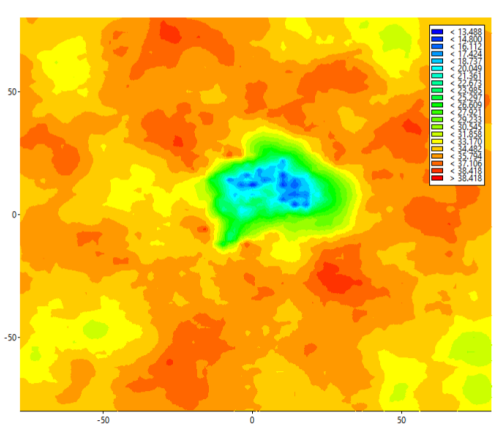

300 K

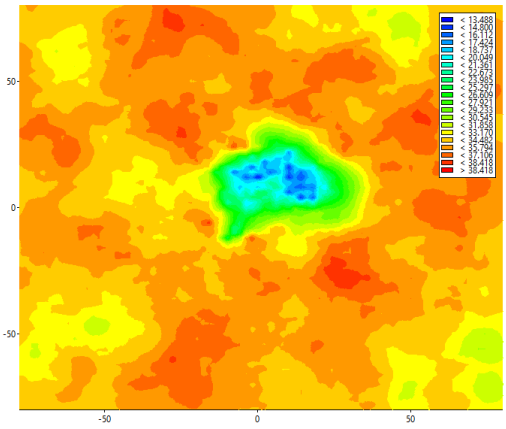

320 K

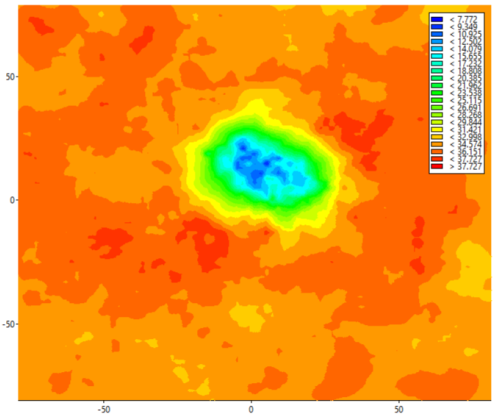

340 K

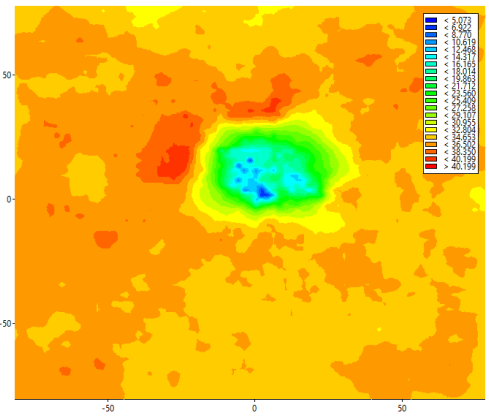

360 K

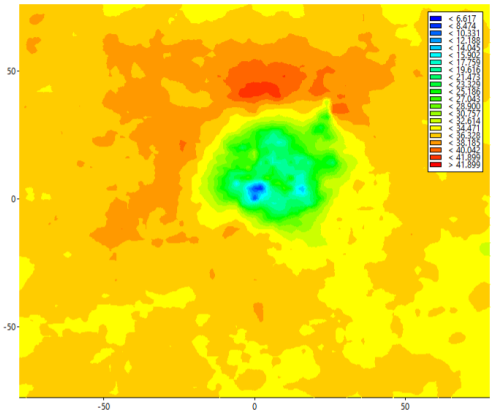

370 K

Figure . S10: Local average thickness of the membrane at different values of temperature for CF1 configuration.

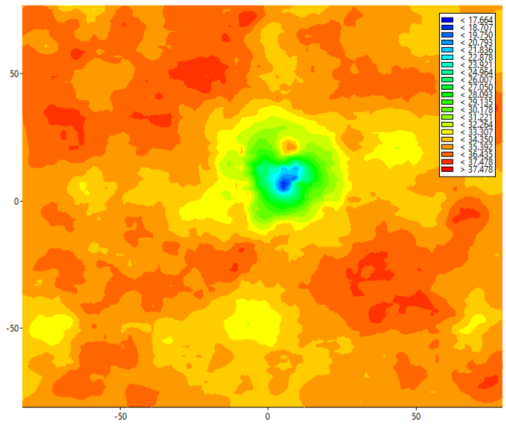

300 K

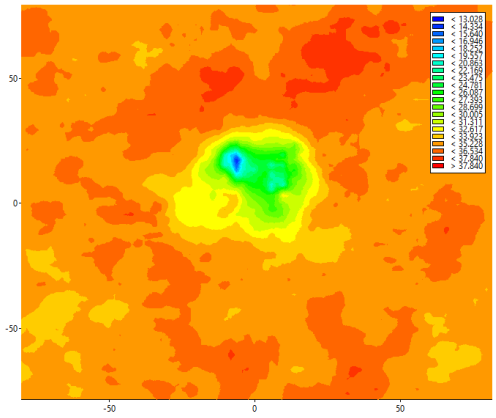

320 K

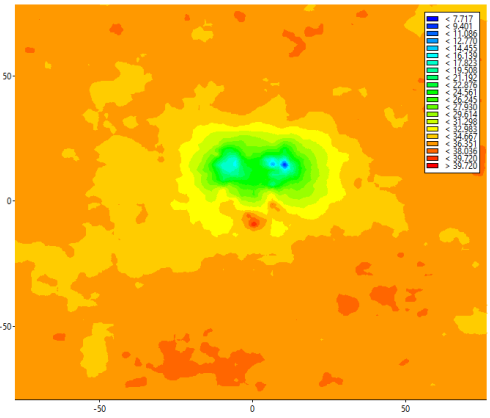

340 K

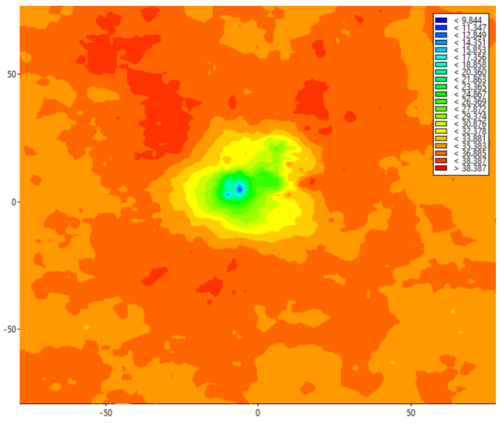

360 K

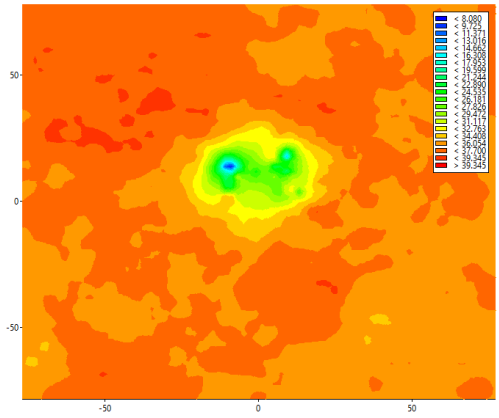

370 K

Figure . S11: Local average thickness of the membrane at different values of temperature for CF2 configuration.

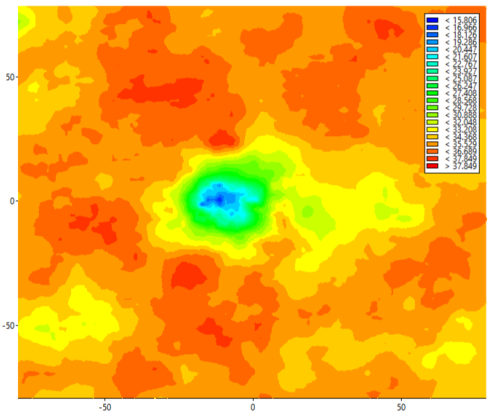

300 K

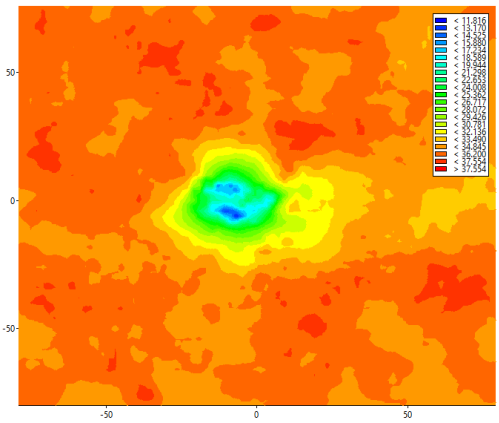

320 K

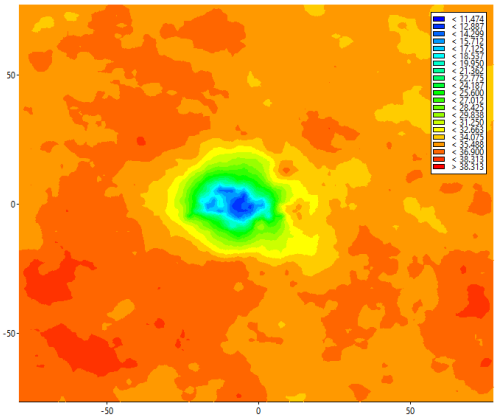

340 K

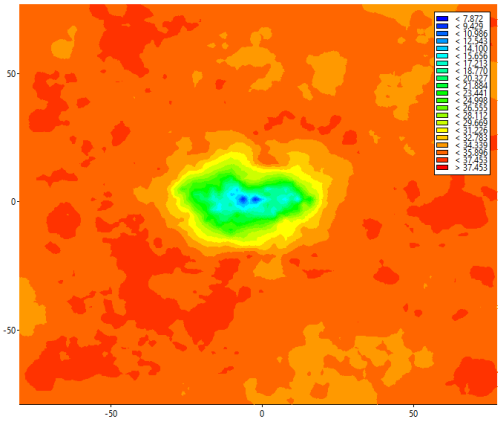

360 K

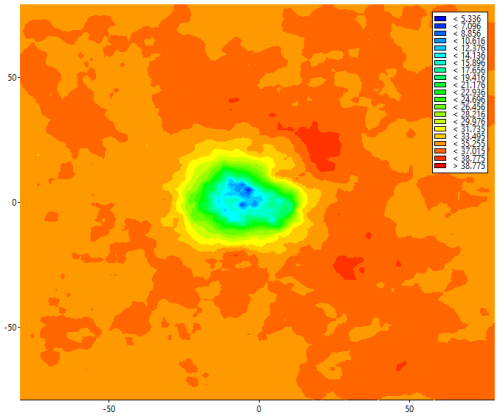

370 K

Figure . S12: Local average thickness of the membrane at different values of temperature for CF3 configuration.